Oceanographic Setting

Brian Kinlan[1,2], Matthew Poti[1,2] and Charles Menza[1,3]

4.1. SUMMARY

In this chapter data on several dynamic oceanographic variables, including water column stratification, sea surface temperature (SST), surface chlorophyll, surface turbidity, and near-surface zooplankton biomass are compiled for the New York study area (Figure 1.2). Data are gridded to a common 30 arc-second resolution and long-term average (climatological) ocean conditions are mapped by season (spring [Mar-May], summer [Jun-Aug], fall [Sep-Nov], winter [Dec-Feb]).These datasets are intended to quantify spatial variation in long-term average patterns of physical and biological oceanographic variables.

Image 4.1. The ocean is a dynamic environment. Photo credit: Edward Moran

4.2. BACKGROUND

The hydrography of the study area is characterized by a strong seasonal cycle, considerable freshwater runoff, and interactions among three distinct large-scale water masses. These water masses produce strong spatial and temporal heterogeneity in both biological and physical parameters, and define biogeographic regions that are often clearly delimited by temperature and/or salinity fronts, although the exact position of these fronts shifts seasonally and inter-annually. Over the shelf, water is relatively cold and fresh, and comes from the Labrador Current via a continuous equatorward coastal current system (Chapman and Beardsley, 1989). The northward-flowing warm equatorial waters of the Gulf Stream pass farther offshore. Between these two and over the slope lies a water mass, commonly called Slope Water, which is a mixture of shelf water and the Gulf Stream.

The frontal boundary between shelf and slope masses is highly dynamic and changes due to wind forcing, gravitational flow, and large scale alterations in atmospheric circulation patterns such as those associated with the North Atlantic Oscillation (NAO) (Pershing et al., 2001). Changes in the relative position of these water masses not only affect physical parameters, such as water temperature, but also species distributions. For instance an infamous 1882 tilefish kill offshore of New Jersey has been attributed to colder-than-usual water temperatures and a low NAO index (Marsh et al., 1999).

Productivity on the shelf is generally nitrogen-limited and therefore is greatest wherever inorganic nitrogen-containing nutrients are supplied, typically by processes such as runoff from rivers and estuaries, turbulent mixing in warm core rings, wind-driven upwelling intrusions of slope water, and intense tidal mixing at shoals. Frontal boundaries and stratification between water masses inhibit mixing, but strong winds, upwelling, and eddies can provide sufficient energy to promote mixing and introduce nutrients. Upwelling occurs south of Long Island during periods of southwesterly winds and during the passage of storms (Walsh et al., 1978). Warm core rings resulting from Gulf Stream meanders occur, but are less frequent than at George's Bank (Ingham et al., 1982).

The shelf's water column stratifies in the spring and summer from warming and freshwater inputs. Stratification isolates warm, well-mixed surface water from cold deeper water and deprives the upper (euphotic) zone of nutrients. During stratification, primary productivity is highest nearshore where periodic coastal upwelling and

[1] Center for Coastal Monitoring and Assessment, National Centers for Coastal Ocean Science, National Ocean Service, National Oceanic and Atmospheric Administration
[2] Consolidated Safety Services, Inc., under NOAA Contract No. DG133C07NC0616
[3] Corresponding author: Charles.Menza@noaa.gov

runoff can provide nutrients. Offshore productivity is limited to the pycnocline where phytoplankton can get nutrients via diffusive fluxes. In late summer, stratification breaks down due to storms and surface cooling. By winter the entire water column over the shelf is well-mixed and a sharp frontal zone separates cold, fresh nearshore water from warmer, more-saline slope water.

4.3. METHODS

In this section, data sources are identified and methods used to interpolate data onto a consistent sampling grid are described. All datasets are co-registered on the same 30 arc-second sampling grid used in Chapters 3 and 6 and clipped to the same study area spatial extent (Figure 1.2). Since sea surface temperature (SST), stratification, chlorophyll, turbidity, and zooplankton biomass are time-varying environmental variables dominated by seasonal variability, long-term average (climatological) ocean conditions were mapped by season (spring [Mar-May], summer [Jun-Aug], fall [Sep-Nov], winter [Dec-Feb]).

Data processing was carried out using ArcGIS 9.3.1 with the Spatial Analyst extension (Environmental Systems Research Group [ESRI], Redlands, CA), Geostatistical Analyst extension (ESRI), XTools Pro 6.2.1 for ArcGIS 9.x (Data East LLC, Novosibirsk, Russia), and Hawth's Tools for ArcGIS 9.x (Beyer, 2004).

Water Column Stratification

Seasonal climatologies of water column stratification were obtained from The Nature Conservancy (TNC) and are described in TNC's Northwest Atlantic Marine Ecoregional Assessment (NAMERA) Phase I Report (Greene et al., 2010; Shumway et al., 2010). Stratification estimates were originally provided to TNC by Dr. Grant Law and subsequently provided to us with permission from the original author (Law, 2011). Briefly, three-dimensional ocean temperature and salinity data were interpolated from a database of conductivity-temperature-depth (CTD) casts, using the OAX5 optimal-analysis algorithm (Hendry and He, 1996). CTD casts came from a compilation of Hydrobase (described in Curry, 1996), NOAA National Marine Fisheries Service databases (described in Mountain, 2003), Fisheries and Ocean Canada databases (described in Gregory, 2004), and South-Atlantic Bight oceanographic data (described in Blanton et al., 2003) (for details see Shumway, 2010 and Law, 2011). Stratification was calculated by subtracting the optimally interpolated seawater density (measured in $kg \cdot m^{-3}$) at 50 meters from the surface seawater density, then averaged to create a 1980 – 2007 climatology (Shumway, 2010). Note that by this definition, stratification is usually negative, corresponding to less dense warmer and/or fresher water occurring on top of more dense colder and/or more saline water. More negative values indicate greater stratification.

The stratification climatology was provided on a 5 arc-minute grid and bi-linearly resampled to the 30 arc-second model grid. We did not explicitly characterize the accuracy of this dataset, but previous accuracy assessments of hydrographic data interpolation in this region suggest relative error on the order of 50% (Taylor and Mountain, 2003). Given this level of uncertainty, and that the original resolution of this dataset is coarser than any of the predictors used in this analysis (spacing between sample points typically 1-10 km or further), this layer should be used with caution for planning scales finer than ~10 km and for any application requiring precise knowledge of stratification at any particular time and place. Better resolution and accuracy might be obtained from more recent data-assimilating numerical ocean models. An improved high-resolution gridded stratification climatology should be a priority for this region.

Stratification in the study area was greatest in the spring and summer (Figure 4.1). In these months, stratification was higher over a broad area of the shelf, decreasing towards the shelf edge and eastwards to Nantucket shoals. In fall, stratification is greatest in the middle of the shelf, with more mixing along shore and to the east and west of the study area. In winter stratification is low compared to other seasons. Relative to the seasonal mean, it is higher nearshore, especially near the Hudson River and east of Long Island Sound.

Sea Surface Temperature (SST)

Seasonal climatologies of sea surface temperature (SST) were obtained by averaging monthly composites from the National Aeronautics and Space Administration (NASA) Pathfinder 1.1 km Advanced Very High Resolution Radiometer (AVHRR) SST archive for the Northwest Atlantic region, 1985-2001 (Wolfteich, 2011), maintained at the University of Rhode Island (URI) and available publicly via OpenDAP (Cornillion et al.,

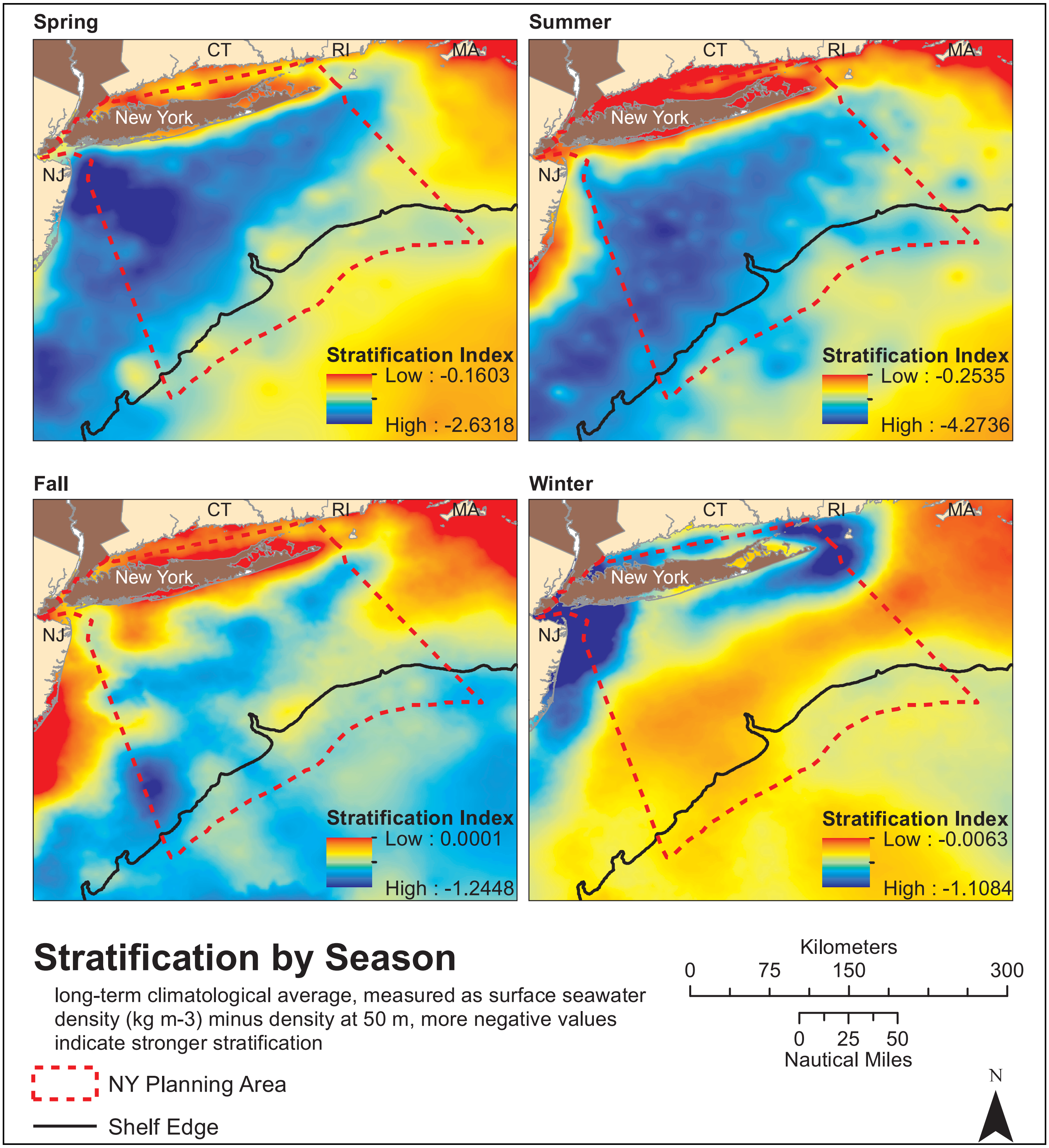

Figure 4.1: Seasonal stratification climatology maps for spring (upper left), summer (upper right), fall (lower left) and winter (lower right). Data courtesy of G. Law (Oregon Health Sciences University), J. Greene (The Nature Conservancy), NOAA Fisheries, Fisheries and Oceans Canada, Woods Hole Oceanographic Institution (Hydrobase), and B. Blanton (University of North Carolina-Chapel Hill).

2003) at the following URL: http://satdat1.gso.uri.edu/opendap/Pathfinder/Northwest_Atlantic/1km/declouded/contents.html. Radiometry data from AVHRR instruments mounted on NOAA satellites was processed using the Pathfinder Algorithm (Casey et al., 2010). Details of the algorithm and processing are provided at the following URL: http://satdat1.gso.uri.edu/opendap/Pathfinder/Pathfinder1km/pathfinder_1km.html

Data were bi-linearly resampled to the 30 arc-second model grid. Given the quality flags that were applied, accuracy of the satellite SST estimates is expected to be approximately ±1° Celsius (about 5% for the range of temperatures in our region) although this can degrade close to land (Casey and Cornillion, 1999). The long time period of averaging resulted in gap-free coverage over the study area except in pixels immediately adjacent to land. SST was generally warmer offshore of the continental shelf break relative to nearshore areas and varied seasonally, with considerable warming of nearshore areas from spring to summer (Figure 4.2). Climatological SST differed little between summer and fall.

Surface Chlorophyll and Turbidity

As a proxy for surface primary productivity, seasonal climatologies of chlorophyll *a* concentration for the period 1998-2006 were extracted from high-resolution (~1.1 km) SeaWiFS satellite data processed using standard NASA ocean biology processing group (OBPG) reprocessing 5.1 algorithms (Franz and Thomas, 2005). Similarly, as a proxy for sea surface turbidity, seasonal climatologies of normalized Lw-670nm for the period 1998-2006 were extracted from the same imagery. All SeaWiFS processing was done by the NOAA Coastal Oceanographic Assessment Status and Trends (COAST) Branch (NOAA/NOS/NCCOS/CCMA/COAST, Silver Spring, MD), following previously

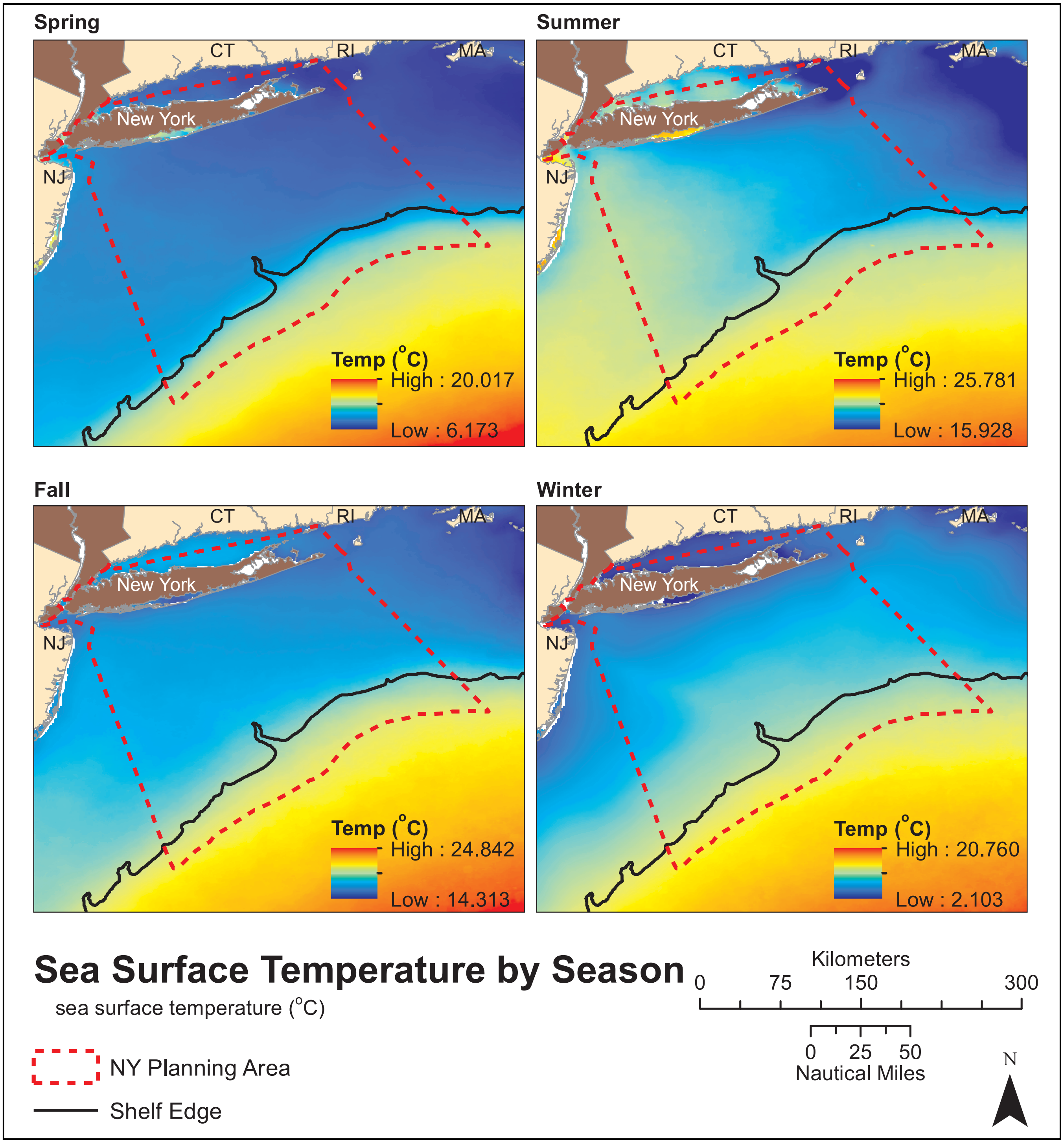

Figure 4.2: Seasonal sea surface temperature climatology maps for spring (upper left), summer (upper right), fall (lower left) and winter (lower right). Data courtesy of C. Wolfriech (University of Rhode Island).

documented methods (Franz and Thomas, 2005; Pirhalla et al., 2009), except a despeckling filter was also applied (Gonzalez and Woods, 1992). Accuracy statistics of ocean color imagery have been reviewed extensively (Franz et al., 2007); under ideal conditions SeaWiFS error tolerances are <5% for water-leaving radiances and <35% for chlorophyll *a*;however, errors can be substantially higher in coastal waters (Franz et al., 2007). The long time period of averaging resulted in gap-free coverage over the study area except in pixels adjacent to land.

Chlorophyll *a* concentrations changed by seasons, but showed similar broad-scale spatial patterns (Figure 4.3). Concentrations were highest in the summer and lowest in the winter. In all months, concentrations were highest neashore and in Long Island Sound and low over most of the shelf and offshore of the continental shelf break. Turbidity showed a similar spatial pattern, but was highest in the spring (Figure 4.4).

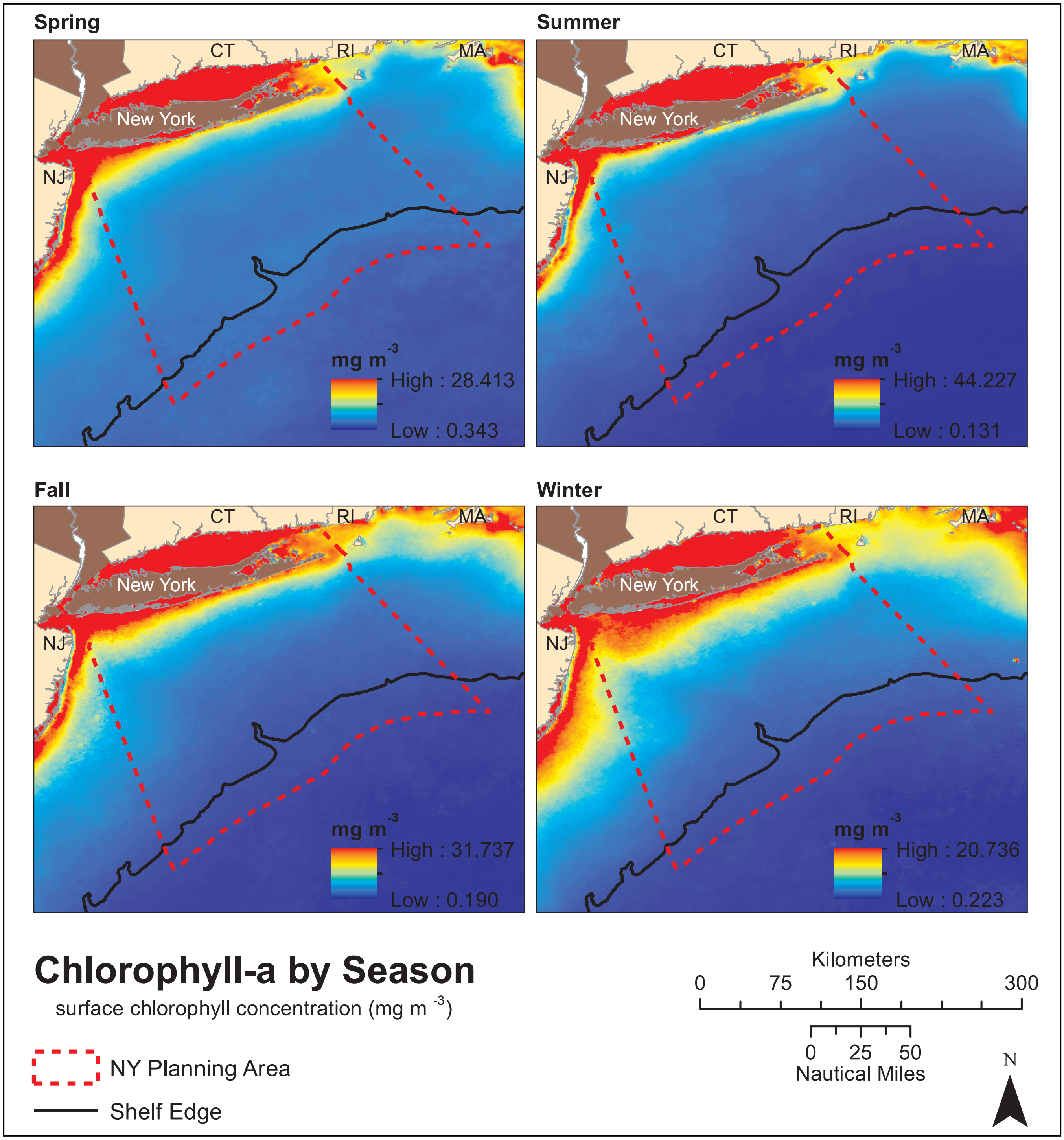

Figure 4.3: Seasonal chlorophyll a climatology maps for spring (upper left), summer (upper right), fall (lower left) and winter (lower right). Data from the Sea-viewing Wide Field-of-view Sensor (SeaWiFS) satellite, processed by D. Pirhalla and V. Ransibrahmanakul (NOAA/NOS/NCCOS/CCMA/COAST). Raw SeaWiFS imagery provided by NASA under research/educational agreement with GeoEye, Inc.

Near-surface Zooplankton Biomass

Point estimates of zooplankton biomass (mean displacement volume per volume of water strained) were obtained from the NOAA National Marine Fisheries Service's (NMFS) Copepod database. The all-taxa zooplankton global compilation was used, available at: http://www.st.nmfs.noaa.gov/plankton/atlas/data_src/copepod-2010__4000000-compilation.txt.

In the study region, we found 3,122 records of zooplankton biomass from 1966-2001. These were grouped by season and processed using ordinary kriging (with locally quadratic detrending) to produce a gridded seasonal climatology at the required resolution. We pooled observations over time to estimate the long-term climatological spatial mean. Ordinary kriging was used because the data exhibited approximately stationary

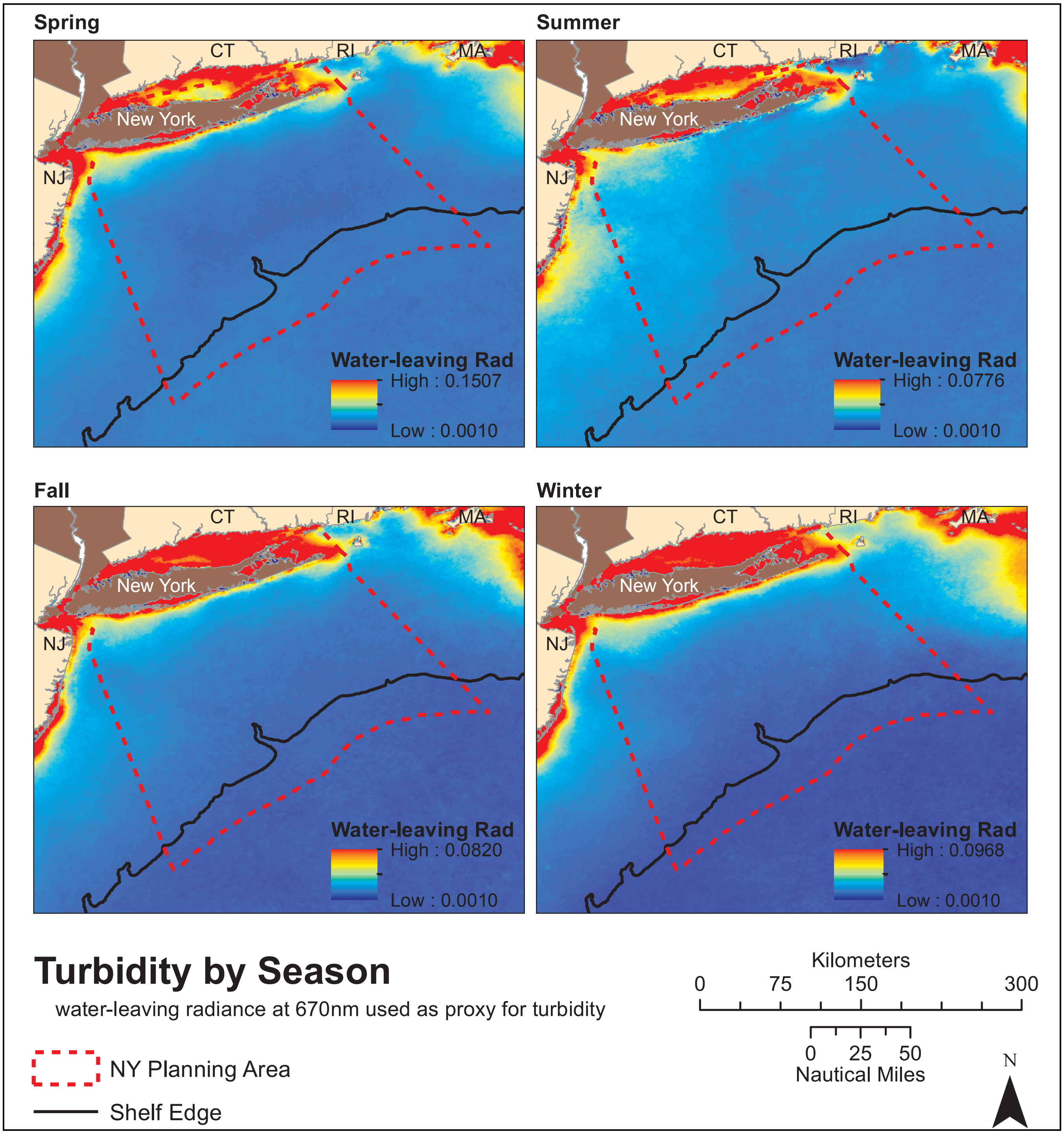

Figure 4.4: Seasonal turbidity climatology maps for spring (upper left), summer (upper right), fall (lower left) and winter (lower right). Water-leaving radiance values are normalized to reflect the fraction of incident light reflected, and thus are dimensionless numbers between 0 and 1. Data courtesy of D. Pirhalla and V. Ransibrahmanakul (NOAA/NOS/NCCOS/CCMA/COAST), imagery was provided by NASA under a research/educational agreement with GeoEye, Inc.

(though geometrically anisotropic) spatial autocorrelation over the study region after trend removal. Ordinary kriging was found to perform better than inverse-distance weighting (IDW) based on leave-one-out cross-validation. Predictions were not made where the variogram model explained <2.5% of the total variance (i.e., areas far from data points). Relative cross-validation RMSE was 27% averaged across all seasons (spring 35%, summer 20%, fall 24%, winter 27%). Geostatistical analyses were carried out using Geostatistical Analyst for ArcGIS 9.3 (ESRI).

Zooplankton biomass was greatest in the fall, with patches of relatively high biomass south of Long Island and outside of the study area offshore of New Jersey (Figure 4.5). In the spring, summer and winter zooplankton biomass was heterogeneously distributed and showed different spatial patterns.

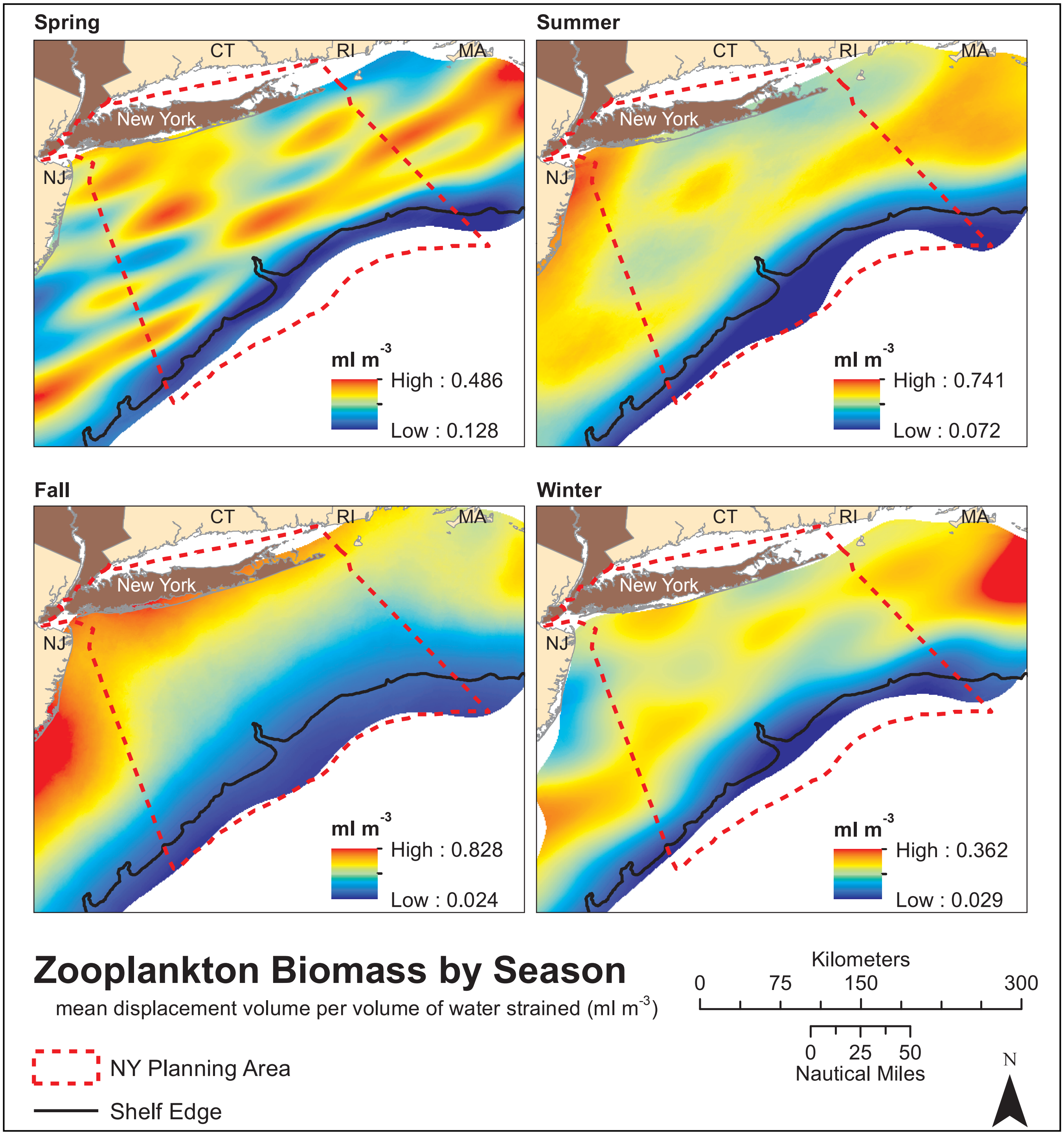

Figure 4.5: Seasonal zooplankton climatology maps for spring (upper left), summer (upper right), fall (lower left) and winter (lower right). Data courtesy of the NOAA National Marine Fisheries Service Copepod database.

4.4. ACKNOWLEDGMENTS

We thank Jenn Greene and Mark Anderson (The Nature Conservancy) and Dr. Grant Law (Oregon Health Sciences University) for providing stratification climatology data, Doug Pirhalla and Varis Ransibrahmanakul (NOAA/NOS/NCCOS/CCMA/COAST Branch) for providing SeaWiFS climatologies, and Carl Wolfteich (URI) for providing 1.1 km Pathfinder SST data. SeaWiFS data are used here for research and educational purposes only in accordance with an agreement between NASA and GeoEye, Inc. (Herndon, VA), which operates the SeaWiFS instrument. The Pathfinder algorithm and data processing steps for AVHRR SST data were originally developed at University of Miami, Rosenstiel School of Marine and Atmospheric Science. Zooplankton data was courtesy of the public NOAA NMFS Copepod database. Brian Calder (University of New Hampshire Center for Coastal and Ocean Mapping) and John Goff (University of Texas at Austin) provided technical reviews that improved this chapter, though any errors or omissions are the sole responsibility of the authors.

4.5 REFERENCES

Beyer, H.L. 2004. Hawth's Analysis Tools for ArcGIS. Available at http://www.spatialecology.com/htools.

Blanton, B.O., A. Aretxabaleta, F. Werner, and H. Seim. 2003. Monthly climatology of the continental shelf waters of the South Atlantic Bight. J. Geophys. Res. 108 (C8): 3264, doi: 10.1029/2002JC001609.

Casey, K. and P. Cornillon. 1999: A comparison of satellite and in situ–based sea surface temperature climatologies. J. Climate 12: 1848–1863.

Casey, K.S., T.B. Brandon, P. Cornillon, and R. Evans. 2010. "The Past, Present and Future of the AVHRR Pathfinder SST Program", in Oceanography from Space: Revisited, eds. V. Barale, J.F.R. Gower, and L. Alberotanza, Springer. DOI: 10.1007/978-90-481-8681-5_16

Chapman, D.C. and R.C. Beardsley. 1989. On the origin of shelf water in the Middle Atlantic Bight. Journal of Physical Oceanography 19(3):384–391.

Cornillon, P., J. Gallagher and T. Sgouros. 2003. OPeNDAP: Accessing Data in a Distributed, Heterogeneous Environment, Data Science Journal 2:164-174.

Curry, R.G. 1996. Hydrobase - A database of hydrographic stations and tools for climatological analysis, Woods Hole Ocenog. Inst. Tech. Rep., WHOI-96-01, 44 pp.

Franz, B.A. and D. Thomas. 2005. Overview of MODIS/Aqua Ocean Color Processing & Distribution. NASA Ocean Biology Processing Group. Online publication. Retrieved from: http://oceancolor.gsfc.nasa.gov/DOCS/MODISA_processing.htm

Franz, B.A., S.W. Bailey, P.J. Werdell, and C.R. McClain. 2007. Sensor-independent approach to the vicarious calibration of satellite ocean color radiometry. Appl. Optics 46:5068–5082.

Gonzalez, R. and R. Woods. 1992. Digital Image Processing. Addison-Wesley Publishing Company. 191 pp.

Greene, J.K., M.G. Anderson, J. Odell, and N. Steinberg, (eds). 2010. The Northwest Atlantic Marine Ecoregional Assessment: Species, Habitats and Ecosystems. Phase One. The Nature Conservancy, Eastern U.S. Division, Boston, MA. URL: http://www.nature.org/ourinitiatives/regions/northamerica/areas/easternusmarine/explore/index.htm.

Gregory, D.N. 2004. Climate: A Database of Temperature and Salinity Observations for the Northwest Atlantic DFO Can. Sci. Advis. Sec. Res. Doc. 2004/075

Hendry, R. and I. He. 1996. Technical Report on Objective Analysis (OA) Project. Unpublished document available at URL: http://www2.mar.dfo-mpo.gc.ca/science/ocean/coastal_hydrodynamics/Oax/download/techrep.ps

Ingham, M.C., R.S. Armstrong, J.L. Chamberlin, S.K. Cook, D.G. Mountain, R.J. Schlitz, J.P. Thomas, J.J. Bisagni, J.F. Paul and C.E. Warsh. 1982. Summary of the Physical Oceanographic Processes and Features Pertinent to Pollution Distribution in the Coastal and Offshore Waters of the Northeastern United States, Virginia to Maine. NEMP Oceanography Summary Report. NEMP-IV-82-C-004. Washington, DC: U.S. Department of Commerce.

Law, G. 2011. Center for Coastal Margin Observation and Prediction, Oregon Health and Science University. Pers. comm., emails with B. Kinlan, C. Menza, and M. Poti, March 2011 – August 2011.

Marsh, R.B., B. Petrie, C.R. Weidman, R.R. Dickson, J.W. Loder, C.G. Hannah, K. Frank and K. Drinkwater. 1999. The 1882 tilefish kill – a cold event in shelf waters off the north-eastern United States? Fish. Oceanography 8:39-49.

Mountain, D.G. 2003. Variability in the properties of Shelf Water in the Middle Atlantic Bight, 1977–1999. J. Geophys. Res. 108, NO. C1, 3014, doi:10.1029/2001JC001044.

Pershing, A.J., C.H. Greene, C. Hannah, D. Sameoto, E. Head, D.G. Mountain, J.W. Jossie, M.C. Benfield, P.C. Reid, and T.G. Durban. 2001. Oceanographic responses to climate in the Northwest Atlantic. Oceanography 14:76-82.

Pirhalla, D.E., V. Ransibrahmanakul, and R. Clark. 2009. An Oceanographic Characterization of the Olympic Coast National Marine Sanctuary and Pacific Northwest: Interpretive Summary of Ocean Climate and Regional Processes Through Satellite Remote Sensing. NOAA Technical Memorandum NOS NCCOS 90. Silver Spring, MD. 55 pp.

Shumway, C., K. Ruddock, and M. Clark. 2010. Physical Oceanography. Chapter 4 In: Greene, J.K., M.G. Anderson, J. Odell, and N. Steinberg (eds.). The Northwest Atlantic Marine Ecoregional Assessment: Species, Habitats and Ecosystems. Phase One. The Nature Conservancy, Eastern U.S. Division, Boston, MA.

Taylor, M.H. and D. Mountain. 2003. The role of local wintertime atmospheric heat flux in determining springtime temperature variability in the northern Middle Atlantic Bight during 1965–1973. Continental Shelf Research 23:377–386.

Walsh, J.J., T.E. Whitledge, F.W. Barvenik, C.D. Wirick, and S.O. Howe. 1978. Wind events and food chain dynamics within New York Bight. Limnol. Oceanogr. 23:659-683.

Wolfteich, C. 2011. Web document: URI/NASA AVHRR Pathfinder 1km SST Archive. Retrieved April 2011 from http://satdat1.gso.uri.edu/opendap/Pathfinder/Pathfinder1km/pathfinder_1km.html